Carbon doping of superconducting magnesium diboride

R.A. Ribeiro [*], S.L. Bud'ko, C. Petrovic, P.C. Canfield

Ames Laboratory and Department of Physics and Astronomy
Iowa State University, Ames, IA 50011 USA

Abstract

We present details of synthesis optimization and physical properties of nearly single phase carbon doped MgB_2 with a nominal stoichiometry of $Mg(B_{0.8}C_{0.2})_2$ synthesized from magnesium and boron carbide (B_4C) as starting materials. The superconducting transition temperature is ≈ 22 K (≈ 17 K lower than in pure MgB_2). The temperature dependence of the upper critical field is steeper than in pure MgB_2 with $H_{c2}(10K) \approx 9$ T. Temperature dependent specific heat data taken in different applied magnetic fields suggest that the two-gap nature of superconductivity is still preserved for carbon doped MgB_2 even with such a heavily suppressed transition temperature. In addition, the anisotropy ratio of the upper critical field for $T/T_c \approx \frac{2}{3}$ is $\gamma \approx 2$. This value is distinct from 1 (isotropic) and also distinct from 6 (the value found for pure MgB_2).

Key words: magnesium diboride, carbon doping, synthesis, physical properties
PACS: 74.70.Ad, 74.62.Dh, 74.25.-q

1 Introduction

Since the discovery of superconductivity in magnesium diboride at elevated ($T_c \approx 40$ K) temperature [1,2], considerable progress has been achieved in material synthesis as well as in understanding of its physical properties [3,4,5,6,7,8]. From these initial days of research on superconducting MgB_2 many attempts were made to tailor the physical properties of the material to suite different needs as well as to explore the neighboring compounds in search of even higher T_c values.

---

[*] Corresponding author.
 Email address: `ribeiro@ameslab.gov` (R.A. Ribeiro).

A number of groups undertook synthesis and characterization of $(Mg_{1-z}T_z)B_2$ or $Mg(B_{1-y}M_y)_2$ (T = transition metal, Li, Be, Al; M = C, Si) materials. The agenda was multi-fold: to look for changes in T_c, to perform tests of the superconducting mechanisms in MgB_2, and to introduce additional pinning centers that could lead to higher critical current densities. Since many diborides crystallize in the same, hexagonal AlB_2 type of structure as MgB_2, and these compounds have been known and studied for decades [9] these substitutions initially were viewed as feasible. In spite of considerable efforts, substitutions in MgB_2 appeared to be difficult and in many cases unsuccessful or, at best, ambiguous.

For magnesium site substitutions apparently only Al was shown to enter the structure unambiguously [10,11,12,13,14] although in a limited concentration range. For boron site substitutions a number of attempts with different elements were made. Carbon substitution was reported in several publications [15,16,17,18,19,20]. Most of these attempts had elemental magnesium, boron and carbon as starting materials and the synthesis was performed at different pressures and temperatures. The results varied considerably depending on the details of sample synthesis (for uniformity we refer to the chemical formula written as $Mg(B_{1-x}C_x)_2$): carbon solubility less then 1.25% was reported in [15], a two-step transition was observed in resistance measurements for nominal $x = 0.1$ [16], a solubility limit of approximately $x = 0.35$ and shift of T_c down to ≈ 34.8 K for $x = 0.03$ was reported in [17], a T_c value of 34 K (at 2% of full diamagnetic signal, $\Delta T_c = 3K$) was measured by DC magnetization at 20 Oe in $Mg(B_{0.8}C_{0.2})_2$ (with no mention of solubility limit) in [19], and a solubility limit of $x \approx 0.15$ and $T_c(x = 0.15) \approx 30$ K was determined from magnetic measurements in [20].

One of the difficulties associated with doping of MgB_2 may be the fact that the MgB_2 structure is robust and an intimate, atomic level, mixing of the dopant with the doped element before or in the process of synthesis is required to achieve the substitution. An interesting approach for carbon doping of MgB_2 was suggested by Mickelson *et al.* [18]. The starting materials for synthesis were elemental magnesium and boron carbide (B_4C) powder. The result of their synthesis was carbon doped MgB_2 as a majority phase and MgB_2C_2 as a minority phase. The T_c of the material was decreased by 7 K (down to 32 K) as seen by magnetization and resistance measurements. The resulting composition of the sample was estimated to be $Mg(B_{0.9}C_{0.1})_2$. This initial study motivated us to attempt to optimize this synthetic route so as to eliminate the impurity phases and to perform a thorough investigation of the physical properties of the resulting material.

2 Experimental

Samples of carbon doped MgB_2 for this study were synthesized in the form of sintered pellets following the procedure used for pure MgB_2 [3,4,21]. Magnesium lumps (99.9%) and B_4C powder (99% - Alfa Æsar) were sealed into tantalum tubes, sealed in quartz, placed into a heated box furnace and then (after the desired synthesis time) quenched to to room temperature. For all the samples except one ($MgB_2C_{0.5}$), the nominal stoichiometry was kept as $Mg(B_{0.8}C_{0.2})_2$, i. e. $Mg_5(B_4C)_2$. Synthesis temperature and time were varied systematically so as to optimize sample quality.

Powder X-ray diffraction (XRD) measurements were made at room temperature using Cu K_α radiation in a Scintag diffractometer. A Si standard was used for all runs. The Si lines were removed from the X-ray diffraction data leading to the apparent gaps in the powder X-ray data. The lattice parameters were obtained by fitting the X-ray diffraction spectra using *Rietica* software.

DC magnetization measurements were performed in Quantum Design MPMS-5 and MPMS-7 SQUID magnetometers. Four-probe AC resistance measurements were carried out in Quantum Design MPMS (with external LR-400 and LR-700 resistance bridges) and PPMS-9 units. Platinum wires were attached to the samples with Epotek H20E silver epoxy. Heat capacity data was collected on small pressed pellet samples using the PPMS-9 instrument in an applied field of up to 9 T utilizing the relaxation technique.

3 Synthesis Optimization

Figure 1a presents low field magnetization data for a nominal $Mg(B_{0.8}C_{0.2})_2$ sample that was synthesized by heating for two hours at 600°C and then for two more hours at 700°C. This sample was made using the temperature/time schedule outlined by Mickelson *et al.* [18] and serves as a point of comparison. T_c of this sample (defined via the onset of diamagnetism criterion) is ≈ 30.5 K and the superconducting fraction is significantly less than 100 %. Temperature dependent resistance for this sample is shown in the inset of Fig. 1a. The resistive transition temperature is consistent with the one determined by magnetic measurements. The residual resistance ratio $RRR = R(300K)/R_0 \approx 5.5$ (with R_0 defined, in this case, as normal state resistance just above the transition). Powder X-ray diffraction (see Fig. 1b) confirmed that the $Mg(B_{1-x}C_x)_2$ phase was formed, however three other phases, Mg_2C_3, MgB_2C_2 and remnants of B_4C were also detected. Although the T_c of this sample is comparable with the one reported by Mickelson *et al.* [18], it appears to be poorly formed and clearly requires optimization.

The presence of unreacted B_4C in the X-ray pattern indicates that the reaction is probably not complete. Our next step in optimization was to increase the reaction time to 24 hours and to perform synthesis at number of different temperatures. Figure 2 presents powder X-ray diffraction spectra for nominal $Mg(B_{0.8}C_{0.2})_2$ samples synthesized for 24 hours at four different temperatures: 750°C, 950°C, 1100°C, and 1200°C. Whereas the 750°C/24h sample contains a considerable amount of unreacted B_4C, traces of B_4C are much smaller for the 950°C/24h sample and are not visible in the XRD patterns of the 1100°C/24h and 1200°C/24h samples. In addition the amount of the two other impurity phases (Mg_2C_3 and MgB_2C_2) clearly decrease with an increase in synthesis temperature (see Fig. 2). The XRD patterns for 1100°C/24h and 1200°C/24h are very similar with respect to the apparent quantities of the impurity phases and present a significant improvement in purity in comparison to the 750°C/24h and 950°C/24h samples as well as to the sample reported in ref. [18] and data presented in Figure 1. The reactions carried out either at 1100°C or 1200°C appear to be approaching single phase.

Low field DC magnetization and zero field resistance data taken for the same set of samples also show an evolution of physical properties with the synthesis temperature (Fig. 3). The superconducting transition for the 750°C/24h sample has an onset of the diamagnetic signal at 29 K but the transition, in fact, is very broad that probably reveals a distribution of transition temperatures within the sample probably due to chemical inhomogeneities. The transitions as seen in the $M(T)$ data sharpen with the increase of the reaction temperature. The onset temperatures of the diamagnetic signal at the superconducting transition seem to decrease with the increase of the reaction temperature (see Fig. 3a, inset), however the temperatures at which the majority of the sample becomes superconducting (50% of the transition or maximum in $\partial M/\partial T$ points) increase with the synthesis temperature for 950°C/24h - 1200°C/24h samples. Resistance data (Fig. 3b) manifest a similar trend e.g. the transition width decreases with the increase of reaction temperature. The transition temperatures defined using $R = 0$ criterion are 27, 19, 21, and 21.5 K for reaction temperatures of 750°C, 950°C, 1100°C, and 1200°C respectively. RRR decreases from 4.2 to 1.4 with the increase of the reaction temperature.

At this point we attempt (with some hesitancy) to estimate the room temperature resistivity or these samples. Very rough evaluation results in the values: 0.3 mΩ-cm, 0.4 mΩ-cm, 2 mΩ-cm and 2 mΩ-cm for 750°C/24h, 950°C/24h, 1100°C/24h, and 1200°C/24h samples respectively. These numbers present the *apparent* resistivity, with an understanding that (i) the porosity of the samples was not taken into account, (ii) no attempt was made to account for the possible contributions to the measured resistivity value from grain boundaries and impurity phases. Whereas the porosity of different samples prepared by the route described above can be considered as similar and allow for relative comparison of resistivities, we suggest that the possible effects of grain bound-

aries and impurity phases cannot be reliably accounted for within the available data on $Mg(B_{1-x}C_x)_2$ compounds and the minority phases encountered in them. Only gross, order-of-magnitude, changes in apparent resistivity may, with some reservations, be taken as reflecting the real evolution of transport properties. Keeping this warning in mind we compare the apparent room temperature resistivities of nearly single phase nominal $Mg(B_{0.8}C_{0.2})_2$ 1100°C/24h and 1200°C/24h compounds (2-3 mΩ-cm) with those measured on pellets of pure MgB_2 (0.02-0.03 mΩ-cm [22]) synthesized by similar technique using isotopically pure boron. In addition it should be mentioned that the apparent resistivity for MgB_2 synthesized using only 90% pure boron [21] was estimated to be 0.1 mΩ-cm (these samples have $RRR \approx 1.8$, similar to carbon doped 1100°C/24h and 1200°C/24h compounds). In addition, no literature reports on bulk, nominally pure MgB_2 prepared by different techniques report a room temperature resistivity value above several tenths of a mΩ-cm. Based on these comparisons we conclude that our nearly single phase nominal $Mg(B_{0.8}C_{0.2})_2$ has a room temperature resistivity that appears to be significantly higher than pure MgB_2. Any conclusion beyond this fairly gross, qualitative statement runs the risk of over interpreting these data.

Since in a number of applications synthesis at lower temperatures can be beneficial and because the details of the reaction between elemental Mg with B_4C are not known, we have checked to see if by performing this reaction at lower temperatures but longer time we can obtain a material of similar or superior quality to the 1100°C/24h - 1200°C/24h samples. X-ray diffraction patterns taken on samples reacted at 950°C for 3 hours, 24 hours and 5 days are shown in Fig. 4. For this reaction temperature the samples tend to improve with increasing reaction time, the intensities of the peaks corresponding to impurity phases monotonically decrease as reaction time increases from 3 h to 24 h to 5 days. The traces of unreacted B_4C are not seen for 950°C/5 days sample but Mg_2C_3 and MgB_2C_2 are still clearly detectable. The quality of this sample (as inferred from XRD data) is approaching that of the sample synthesized at 1100°C or 1200°C for 24 hours (compare Figs. 2 and 4) but is still apparently inferior. Similarly, the low field magnetization (see Fig. 5a) shows a gradual decrease of the width of the transition, indicating more homogenous samples, with the increase of the reaction time. Temperature dependent resistance data (Fig. 5b) follow the same trend: transition width decreases with increases in the reaction time. The resistive transition temperatures (from $R = 0$) are 19, 19, and 18 K for the 3 h, 24 h, and 5 days reaction times. The RRR values decrease from 3 to 1.3 with the increase of the reaction time. On the other hand the transitions seen for all reaction times, even the 950°C/5 days sample, are all significantly broader than those seen for the 1100°C/24 h and 1200°C/24h samples.

Based on the analysis of the two aforementioned data sets, the 1100°C/24h - 1200°C/24h reactions appear to optimize the sample quality. Having this

in mind we wanted to address one final synthesis concern: would samples with nominal stoichiometry of $Mg(B_{0.8}C_{0.2})_2$ or $MgB_2C_{0.5}$ be cleaner, i. e. do we get better samples with a Mg:B ratio of 1:2 or a Mg:(B + C) ratio of 1:2? Both types of samples we synthesized following the 1100°C/24h schedule. Powder XRD spectra (Fig. 6) attest to the fact that the $Mg(B_{0.8}C_{0.2})_2$ sample is cleaner. Low field temperature dependent magnetization (Fig. 7) show that the transition temperatures of these two samples are virtually identical with a possibly slightly higher superconducting fraction found for the $Mg(B_{0.8}C_{0.2})_2$ sample. Apparently the change to a $MgB_2C_{0.5}$ initial stoichiometry does not improve the purity of the phase or sharpness of the superconducting transition but does promote unwanted second phases.

To summarize, the analysis of the three sets of samples discussed above (having reaction temperature, reaction time and the Mg : B_4C ratio as variables) we find that within the limitations of our synthesis route the $Mg(B_{0.8}C_{0.2})_2$ samples reacted at 1100°C/24h - 1200°C/24h are the closest to being single phase samples and have sharper superconducting transition as seen in the temperature dependent resistance and low field magnetization data. The transition for these samples has shifted down by ≈ 17 K ($T_c \approx 22$ K) with respect to pure MgB_2. The a-lattice parameter is approximately 1.2% smaller than for pure MgB_2 whereas the c-lattice parameter remains practically unchanged, a trend consistent with previous data [17,18,19,20]. The phase purity of these samples is better than that of the sample reported by Mickelson *et al.* [18] and clearly much better than the sample described in Figure 1. From the resistance data for the two sets of samples (with reaction temperature or reaction time being varied) it appears that the more phase-pure and homogenous samples have lower residual resistance ratios. This observation is opposite to what follows from the Mattheissen's rule and is consistent with significant extrinsic contribution to the normal state resistance (and RRR) from other phases, grain boundaries, etc. that render attempts to use even semiquantitative arguments based on normal state transport properties, e. g. the Testardi correlation [20], for such samples ambiguous. On the other hand, it is fairly clear that the intrinsic resistivity of the $Mg(B_{0.8}C_{0.2})_2$ samples is significantly higher than that of our pure MgB_2 samples [4,5,21].

A serious shortcoming of carbon doping through this (Mg + B_4C) reaction route is that determination of the carbon content in the final sample appears to be a difficult and non-trivial task. In this report we will not attempt to address this issue for our samples and will leave this problem for future work. It should be noted that reliable and accurate quantitative determination of the carbon content (x) and/or *consistent* relation between three parameters: T_c, x and a-lattice parameter (since c is practically constant in all reports) cannot be found in the available literature [15,16,17,18,19,20]. As an aside note we would like to mention that we attempted to dope MgB_2 with silicon and phosphorus through (Mg + B_6Si) and (Mg + $B_{13}P_2$) synthesis routes.

These attempts were apparently not successful and resulted in multiphased compounds with no indication of doping into B site.

4 Physical Properties

Once the best available synthesis route was established, the nearly single phase 1100°C/24h sample was chosen for more detailed measurements of physical properties. Fig. 8 presents the temperature dependent resistance measurements taken in different applied fields up to 9 T (an enlarged region near the superconducting transition in 0 - 9 T field range is shown). Unlike the case of pure MgB_2 samples [4,5,6] practically no magnetoresistance in the normal state was observed. This is consistent with the very low residual resistance ratio, $RRR \approx 1.6$ for this sample and high estimated ρ_0. the magnetotransport data (Fig. 8) together with field and temperature dependent magnetization data (not shown here) were used to determine the upper critical field for this sample (Fig. 9). The irreversibility line (H_{irr}) shown in this figure was determined from $M(H)$ loops taken at different temperatures. The irreversibility field for this sample is quite low: it extrapolates to $H_{irr}(0) \approx 2$ T, which probably points to the fact that the carbon substitutions in the sample prepared from the Mg and B_4C mixture at 1100°C/24h conditions do not significantly increase the pinning. On the other hand, the $H_{c2}(T)$ slope for this sample is considerably steeper than in pure MgB_2 (see Fig. 9, inset), so although T_c of the carbon doped sample is approximately half of that for pure MgB_2, the extrapolation $H_{c2}(T \rightarrow 0)$ will give the value close to 16 T, similar to that of high purity MgB_2 [6]. Fig. 10 presents the critical current density for the 1100°C/24h sample as determined from magnetization loops using the Bean model [23]. The critical current densities are quite low, $J_c(1.8K, H=0) \approx 30$ kA/cm^2, which is consistent with low pinning and the low lying irreversibility line (Fig. 9).

The heat capacity of the 1100°C/24h nominal $Mg(B_{0.8}C_{0.2})_2$ sample was measured on two different pressed pellets, from two separate batches in zero and 9 T applied field. The specific heat jump at the superconducting transition is clearly seen (Fig. 11, inset) and the value of the jump is estimated as $\Delta C \approx$ 23 mJ/mol K. From 9 T measurements the electronic term in specific heat is extrapolated to $\gamma \approx 1.9$ mJ/mol K^2 and the Debye temperature is estimated as $\Theta_D \approx 685$ K. Both γ and Θ_D values are lower than those accepted in the literature for pure MgB_2 samples [3,24,25,26] and have the same trend as seen experimentally in [20] and theoretically in [27]. At a gross level, the significant decrease in T_c is consistent with lower γ and Θ_D values for the carbon doped sample. The heat capacity difference $\Delta C_p/T = (C_p(H = 0) - C_p(9T))/T$ as a function of temperature for the two different samples is plotted in Fig. 11. Both qualitatively and quantitatively the two sets of data are similar but it is worth

noting that there is some sample-to-sample and measurement-to-measurement variation.

One of the samples was chosen for more detailed measurements in different applied magnetic fields. The results of these measurements are presented in Fig. 12 in the form of $\Delta C_p/T = (C_p(H) - C_p(9T))/T$ as a function of temperature. The shift in the specific heat jump at superconducting transition is a manifestation of the upper critical field and is consistent with $H_{c2}(T)$ measured by other techniques (see stars in Fig. 9). The more interesting feature appears to be the low temperature shoulder in the excess of specific heat seen in $(C_p(H = 0) - C_p(9T))/T$ data below 10 K (also clearly seen for both samples in the previous figure). A similar feature was observed in pure MgB$_2$ by different groups [24,25,26] and was interpreted as experimental evidence of a second, much lower energy, superconducting gap in MgB$_2$ [24,25,26,28]. There are other important similarities between heat capacity data of pure magnesium diboride and the carbon doped sample: the low temperature feature disappears (lower gap is quenched) in small (0.5 T) applied field and the $\Delta C_p/\gamma T_c$ value is substantially smaller than expected for a BCS superconductors. These two peculiar results were shown to be present in pure MgB$_2$ and to be consequences of the two-gap nature of superconductivity in this material. These similarities in heat the capacity data of pure and carbon doped magnesium diboride imply that despite the significantly suppressed T_c and apparently large increase in resistivity, the novel double gap nature of super-condutivity persists in our nominal Mg(B$_{0.8}$C$_{0.2}$)$_2$ samples. It is worth noting whereas there have been estimates of $T_c \approx 20$ K for "isotropic" (single gap) MgB$_2$ [29,30] the case we seem to find for our nominal Mg(B$_{0.8}$C$_{0.2}$)$_2$ appears to be quite different with two distinct gaps. Further research will be required to confirm this initial observation but, as it currently stands, this finding requires that the two superconducting gaps survive quite dramatic perturbations.

Finally, the anisotropic upper critical field for carbon doped MgB$_2$ was evaluated from temperature dependent magnetization measurements following the procedure outlined in [7,8]. Although the feature corresponding to $T_{c2}^{min}(H)$ in $(\partial M/\partial T)\,|_H$ for this sample was slightly broader than for pure MgB$_2$ it was possible to trace H_{c2}^{min} above ≈ 12 K (see Fig. 13). The anisotropy of H_{c2} at $\approx \frac{2}{3}T_c$ is close to 2, i.e. carbon doped MgB$_2$ has apparently less anisotropic H_{c2} than pure compound that may be a result of distortions in the Fermi surface and require additional theoretical/band-structure studies.

5   Conclusions

The synthesis of carbon doped magnesium diboride from magnesium and boron carbide (B$_4$C) with a nominal stoichometry of Mg(B$_{0.8}$C$_{0.2}$)$_2$ was opti-

mized and resulted in nearly single phase material with $T_c \approx 22$ K. Samples obtained by this route have an upper critical field of ≈ 9 T at 10 K and the slope of $H_{c2}(T)$ is much steeper than for pure MgB$_2$. The sample has moderate J_c values pointing out that carbon introduced in the lattice via this synthetic route does not increase pinning significantly. The specific heat data taken in different applied fields suggest that the two gap superconductivity is preserved in the Mg(B$_{0.8}$C$_{0.2}$)$_2$ sample despite the heavily suppressed T_c. In addition whereas there is a significant H_{c2} anisotropy ($\gamma \approx 2$ for $T/T_c \approx \frac{2}{3}$), it is reduced from the anisotropy found in pure MgB$_2$.

6   Acknowledgements

References

[1] J. Akimitsu, Symposium on Transition Metal Oxides, Sendai, January 10, 2001.

[2] J. Nagamatsu, N. Nakagawa, T. Murakana, Y. Zenitani, and J. Akimitsu, Nature **410** (2001) 3.

[3] S.L. Bud'ko, G. Lapertot, C. Petrovic, C.E. Cunningham, N. Anderson and P.C. Canfield, Phys. Rev. Lett. 86 (2001) 1877.

[4] D. K. Finnemore, J. E. Ostenson, S.L. Bud'ko, G. Lapertot and P.C. Canfield, Phys. Rev. Lett. 86 (2001) 2420.

[5] P.C. Canfield, D.K. Finnemore, S.L. Bud'ko, J.E. Ostenson, G. Lapertot, C.E. Cunningham, and C. Petrovic, Phys. Rev. Lett., **86** (2001) 2423.

[6] S.L. Bud'ko, C. Petrovic, G. Lapertot, C.E. Cunningham, P.C. Canfield, M-H. Jung, and A.H. Lacerda, Phys. Rev. B **63** (2001) 220503.

[7] S. L. Bud'ko, V. G. Kogan, and P. C. Canfield, Phys. Rev. B **64** (2001) 180506.

[8] S.L. Bud'ko and P.C. Canfield, Phys. Rev. B **65**, (2002) 212501.

[9] See for example, J. Castaing and P. Costa in *Boron and Refractory Borides* ed. by V.I. Matkovich (Berlin, Heidelberg, New York: Springer-Verlag) (1977) p. 390, and references therein.

[10] J.S. Slusky, N. Rogado, K.A. Regan, M.A. Hayward, P. Khalifah, T. He, K. Inumaru, S.M. Loureiro, M.K. Haas, H.W. Zandbergen, and R.J. Cava, Nature **410** (2001) 343.

[11] B. Lorenz, R.L. Meng, Y.Y. Xue, and C.W. Chu, Phys. Rev. B, **64** (2001) 052513.

[12] J.Q. Li, L. Li, F.M. Liu, C. Dong, J.Y. Xiang, and Z.X. Zhao, Phys. Rev. B, **65** (2002) 132505.

[13] H.W. Zandbergen, M.Y. Wu, H. Jiang, M.A. Hayward, M.K. Haas, and R.J. Cava, Physica C, **366** (2002) 221.

[14] H. Luo, C.M. Li, H.M. Luo, and S.Y. Ding, J. Appl. Phys., **91** (2002) 7122.

[15] M. Paranthaman, J.R. Thompson, and D.K. Christen, Physica C, **355** (2001) 1.

[16] J.S. Ahn, and E.J. Choi, cond-mat/0103169.

[17] T. Takenobu, T. Ito, Dam Hieu Chi, K. Prassides, and Y. Iwasa, Phys. Rev. B, **64** (2001) 134513.

[18] W. Mickelson, J. Cumings, W.Q. Han, and A. Zettl, Phys. Rev. B, **65** (2002) 052505.

[19] Zhao-hua Cheng, Bao-gen Shen, Jian Zhang, Shao-ying Zhang, Tong-yun Zhao, and Hong-wu Zhao, J. Appl. Phys., **91** (2002) 7125.

[20] A. Bharathi, S. Jemina Balaselvi, S. Kalavathi, G.L.N. Reddy, V. Sankara Sastry, Y. Hariharan, and T.S. Radhakrishnan, Physica C, **370** (2002) 211.

[21] R.A. Ribeiro, S.L. Bud'ko, C. Petrovic, and P.C. Canfield, Physica C, **382** (2002) 194.

[22] P.C. Canfield, S.L. Bud'ko, D.K. Finnemore, G. Lapertot, C. Petrovic, C.E. Cunningham, V.G. Kogan, M.-H. Jung, A.H. Lacerda, Studies of High Temperature Superconductors ed. by A.V. Narlikar (2002), v. 38 (Superconducting Magnesium Diboride), 1-24.

[23] C.P. Bean, Phys. Rev. Lett., **8** (1962) 250.

[24] F. Bouquet, R.A. Fisher, N.E. Phillips, D.G. Hinks, and J.D. Jorgensen, Phys. Rev. Lett., **87** (2001) 047001.

[25] Y. Wang, T. Plackowski, and A. Junod, Physica C, **355** (2001) 179.

[26] H.D. Yang, J.-Y. Lin, H.H. Li, F.H. Hsu, C.J. Liu, S.-C. Li, R.-C. Yu, and C.-Q. Jin, Phys. Rev. Lett., **87** (2001) 167003.

[27] N.I. Medvedeva, A.I. Ivanovskii, J.E. Medvedeva and A.J. Freeman, Phys. Rev. B, **64** (2001) 020502.

[28] H.J. Choi, D. Roundy, H. Sun, M.L. Cohen, and S.G. Louie, Nature, **418** (2002) 758.

[29] A.Y. Liu, I.I. Mazin, and J. Kortus, Phys. Rev. Lett., **87** (2001) 087005.

[30] H.J. Choi, D. Roundy, H. Sun, M.L. Cohen and S.G. Louie, Phys. Rev. B, **66** (2002) 020513.
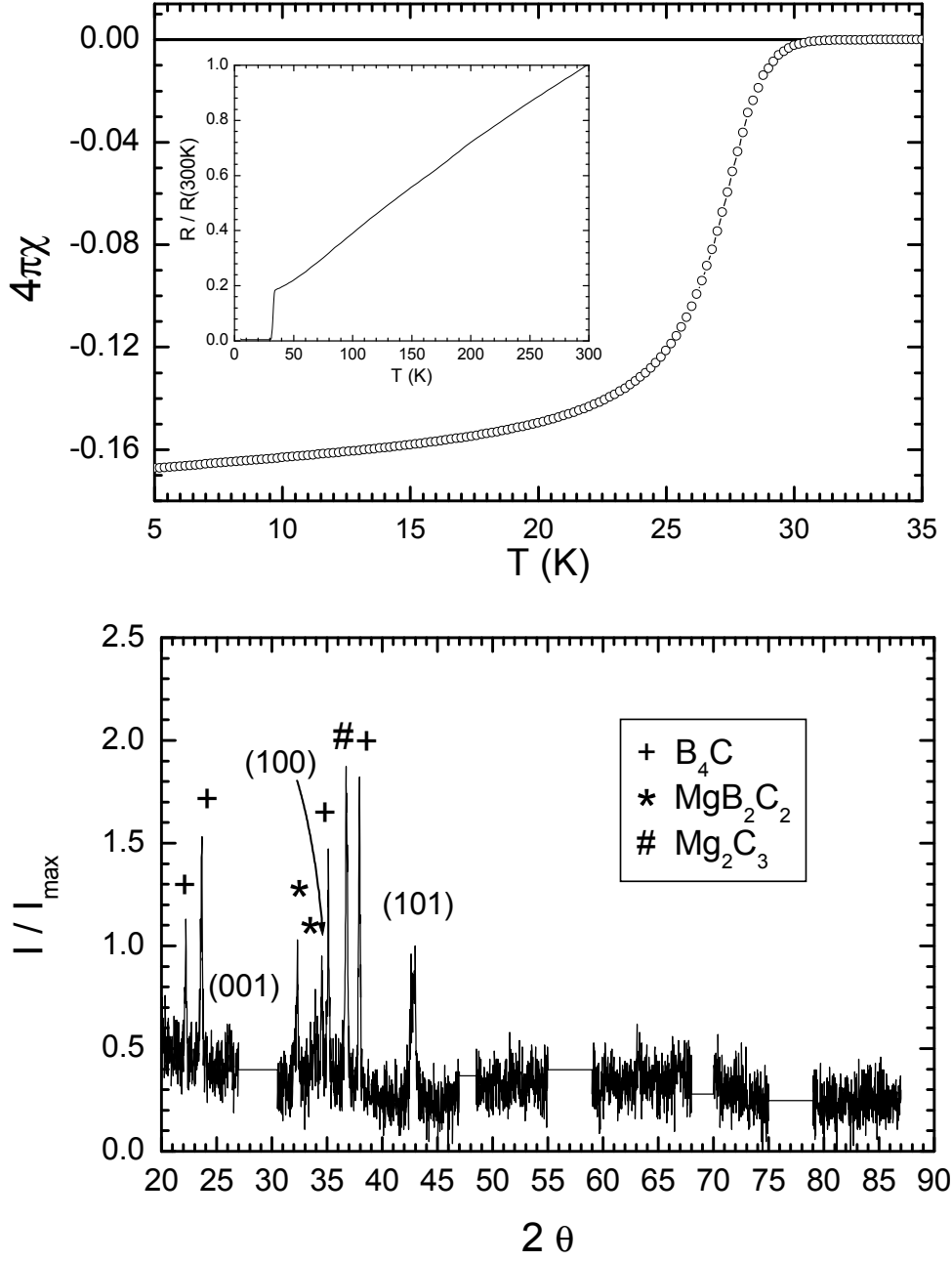
Fig. 1. (a)temperature dependent magnetic susceptibility for $Mg(B_{0.8}C_{0.2})_2$ sample synthesized for 2 h at 600°C and then for 2 h at 700°C taken at $H = 50$ Oe, ZFC - warming, insert - temperature dependent resistance measured in zero applied field; (b) powder X-ray diffraction pattern for the same sample. Numbers in parentheses - (hkl) for $Mg(B_{1-x}C_x)_2$, symbols mark peaks from different impurity phases.
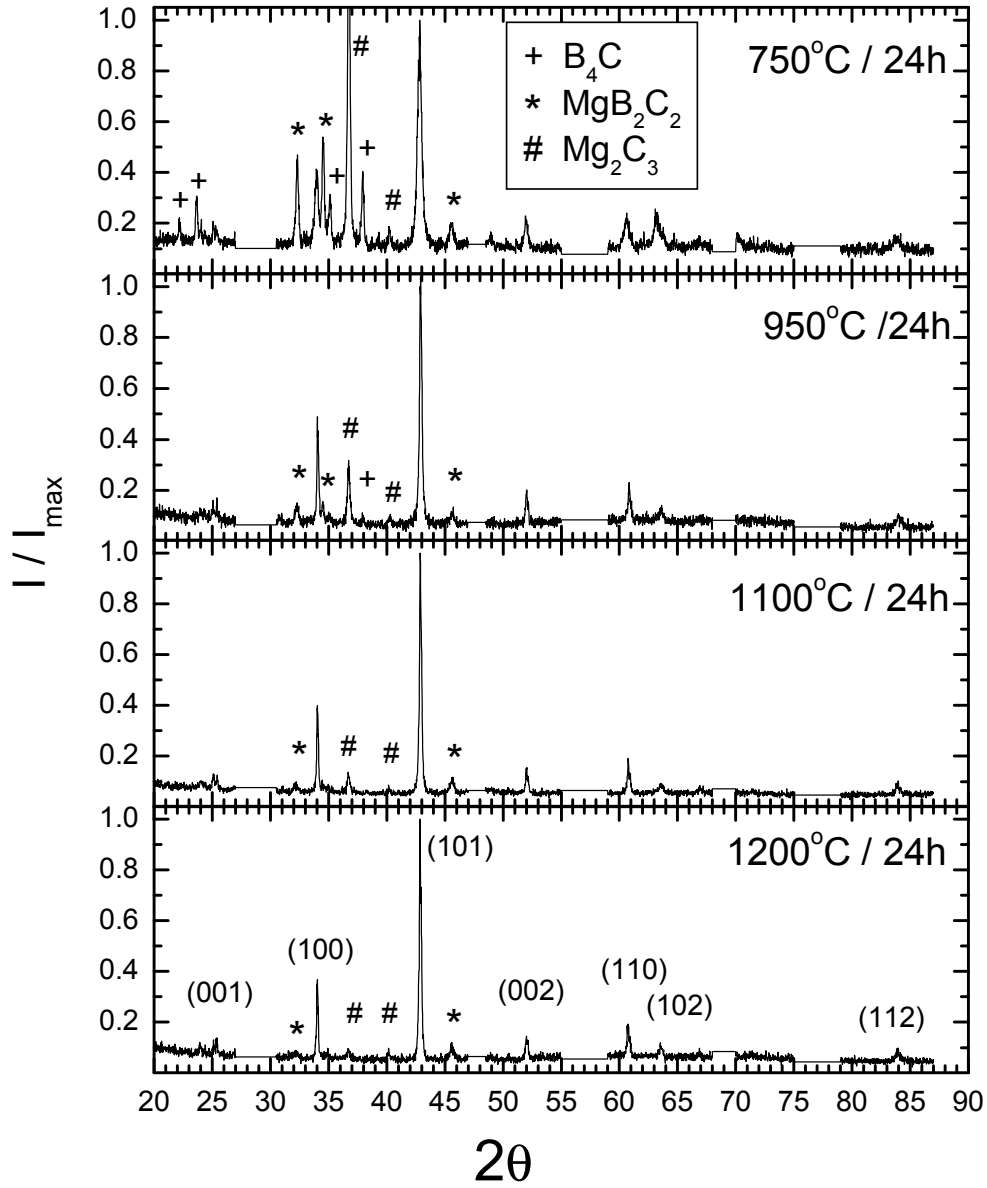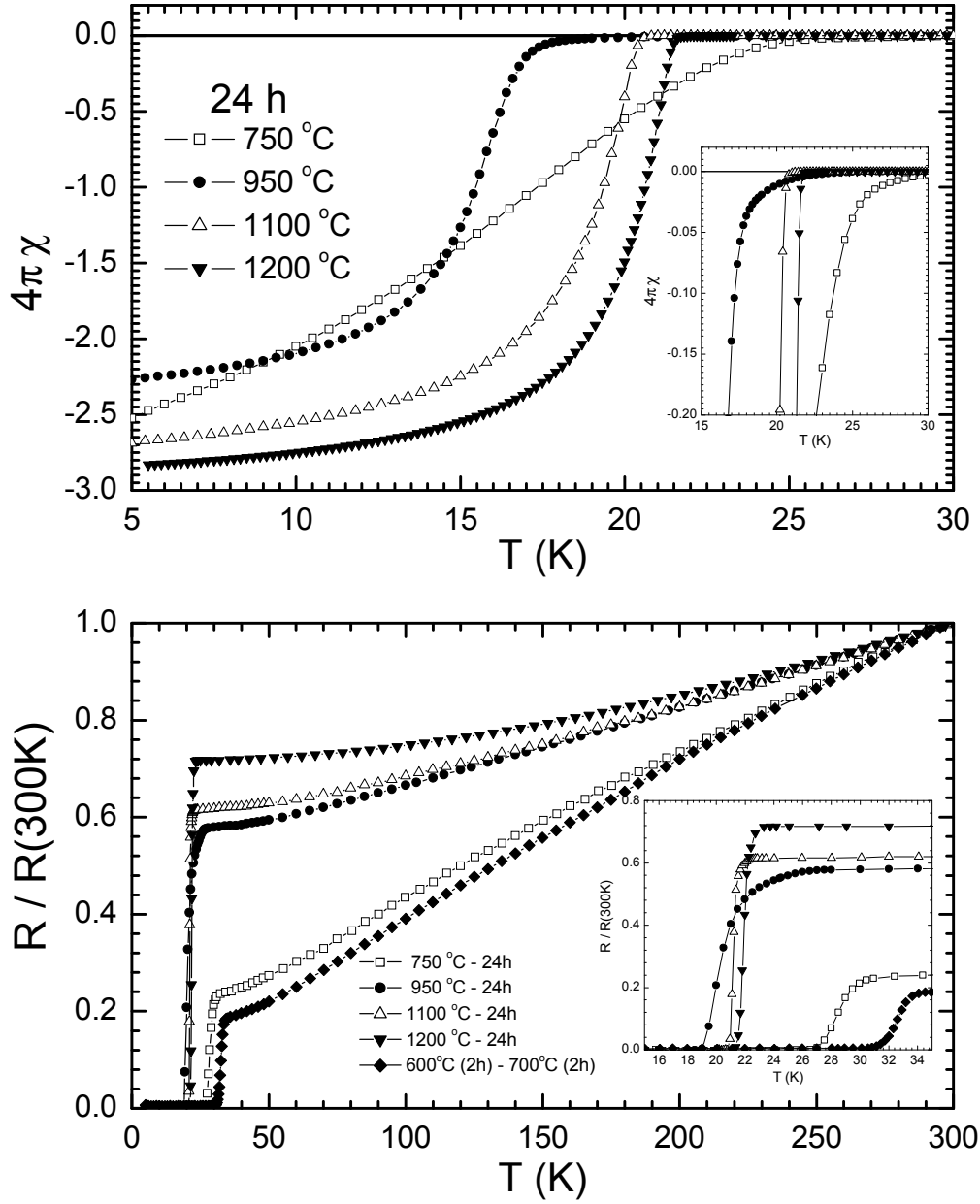
Fig. 2. Powder X-ray diffraction patterns for nominal $Mg(B_{0.8}C_{0.2})_2$ samples synthesized for 24 hours at 750°C, 950°C, 1100°C, and 1200°C. Numbers in parentheses in bottom panel - (hkl) for $Mg(B_{1-x}C_x)_2$, symbols mark peaks from different impurity phases: crosses - B_4C, asterisks - MgB_2C_2, pound signs - Mg_2C_3.

Fig. 3. (a)Temperature dependent magnetic susceptibility for nominal $Mg(B_{0.8}C_{0.2})_2$ samples synthesized for 24 hours at 750°C, 950°C, 1100°C, and 1200°C taken at $H = 50$ Oe, ZFC - warming. Inset: expanded temperature range near T_c. (b)Temperature dependent, normalized resistance for the same set of samples plus reference sample (see text). Inset: expanded temperature range near T_c.
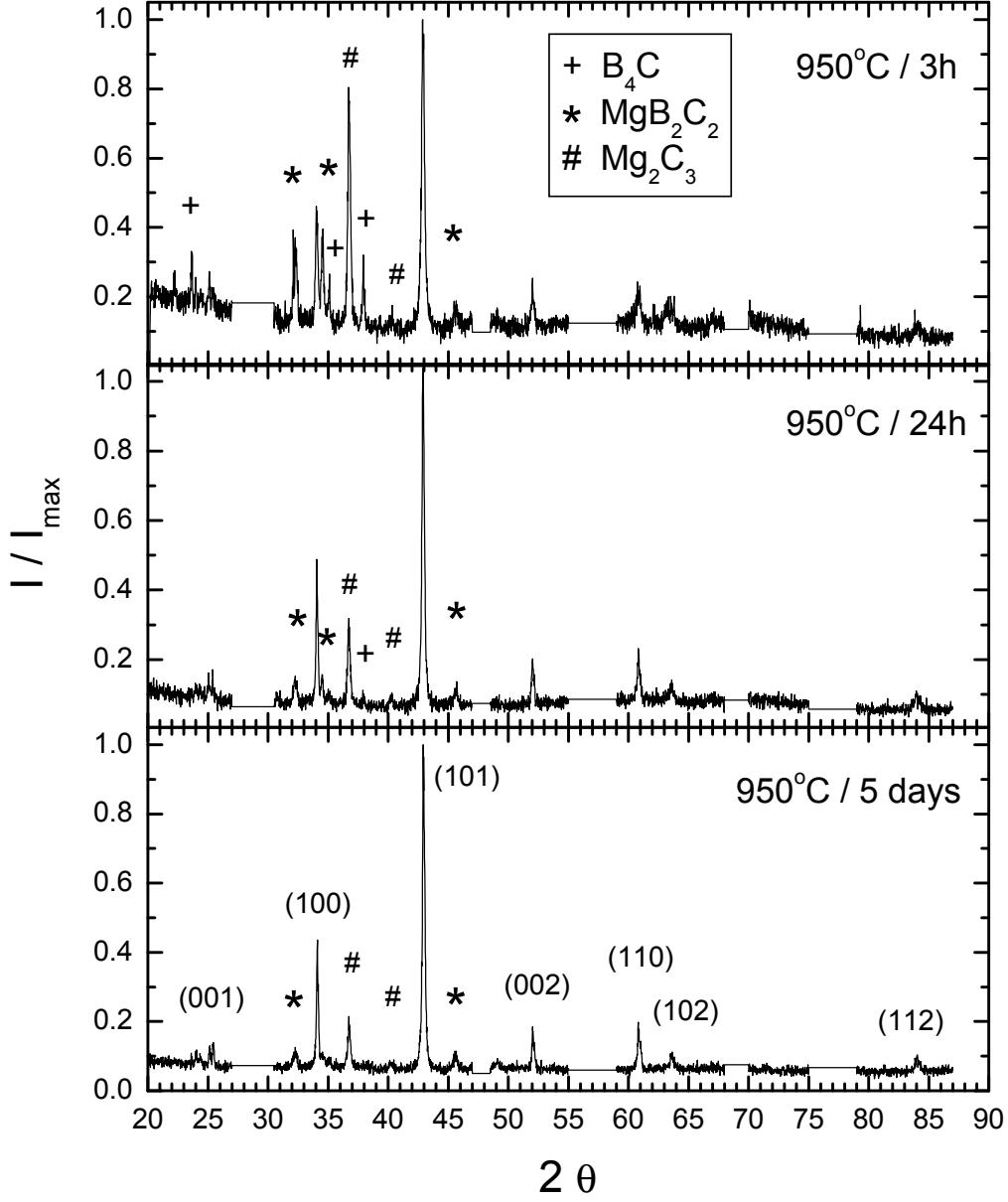
Fig. 4. Powder X-ray diffraction patterns for nominal $Mg(B_{0.8}C_{0.2})_2$ samples synthesized at 950°C for 3 h, 24 h, and 5 days. Numbers in parentheses in bottom panel - (hkl) for $Mg(B_{1-x}C_x)_2$, symbols mark peaks from different impurity phases.

Fig. 5. (a)Temperature dependent magnetic susceptibility for nominal $Mg(B_{0.8}C_{0.2})_2$ samples synthesized at 950°C for 3 h, 24 h, and 5 days. (b)Temperature dependent normalized resistance for the same set of samples. Inset: expanded temperature range near T_c.
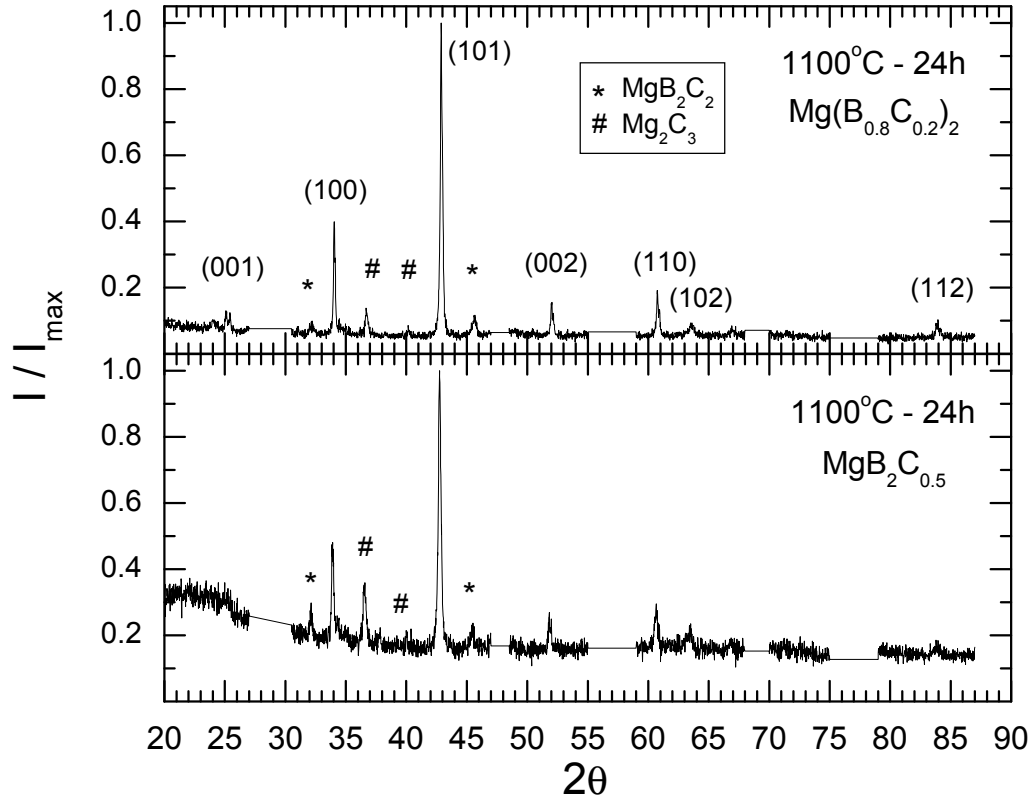
Fig. 6. Powder X-ray diffraction patterns for nominal $Mg(B_{0.8}C_{0.2})_2$ and $MgB_2C_{0.5}$ samples synthesized at $1100°C$ for 24 h. Numbers in parentheses upper panel - (hkl) for $Mg(B_{1-x}C_x)_2$, symbols mark peaks from different impurity phases: crosses - B_4C, asterisks - MgB_2C_2, pound signs - Mg_2C_3.
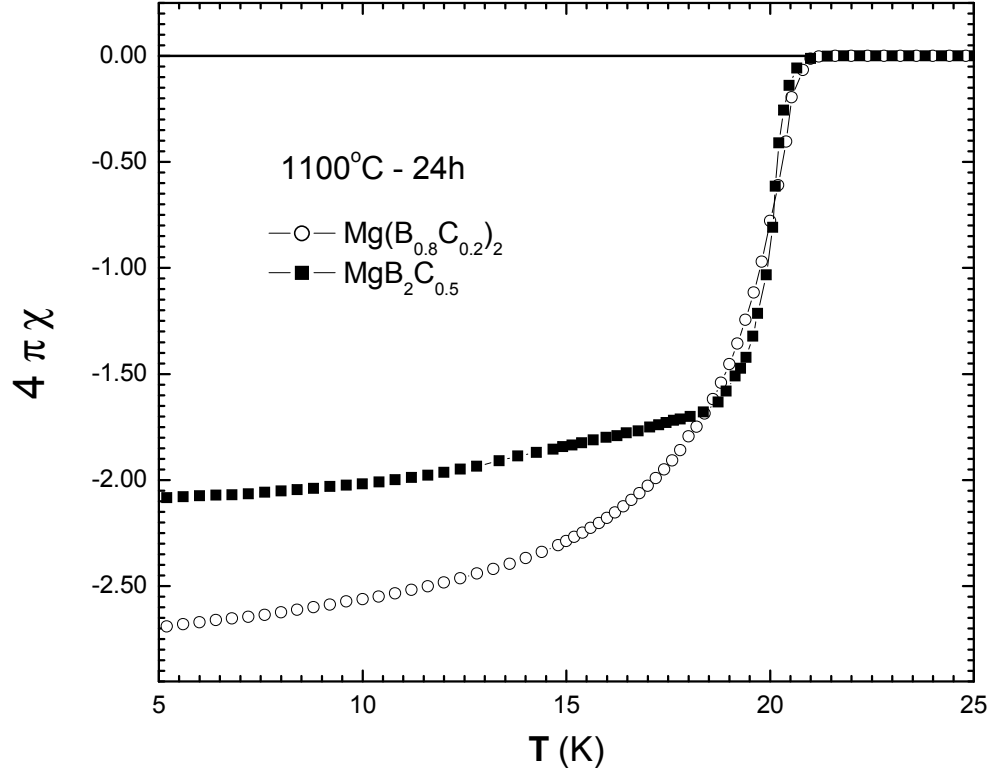
Fig. 7. Temperature dependent magnetic susceptibility ($H = 50$ Oe, ZFC - warming) for nominal $Mg(B_{0.8}C_{0.2})_2$ and $MgB_2C_{0.5}$ samples synthesized at 1100°C for 24 h.
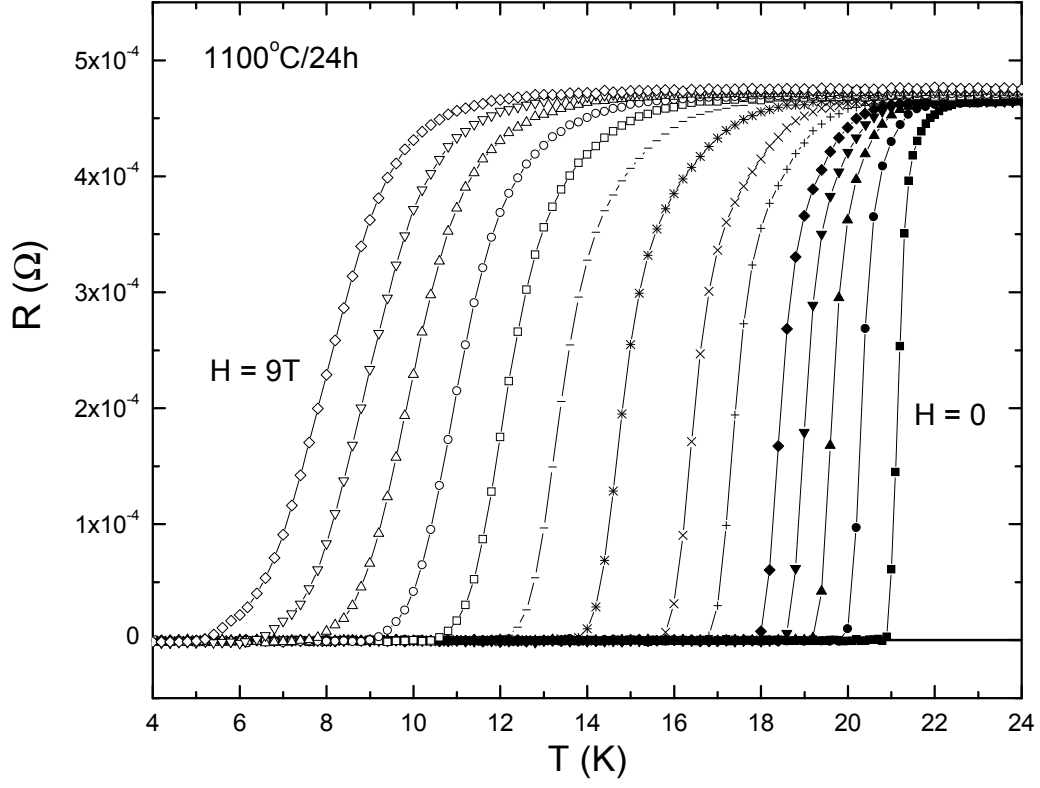
Fig. 8. Temperature dependent resistance for $1100°C/24h$ sample in applied magnetic field (fields from right to left: 0, 0.25, 0.5, 0.75, 1, 1.5, 2, 3, 4, 5, 6, 7, 8, 9 T). Region near the transition shown.
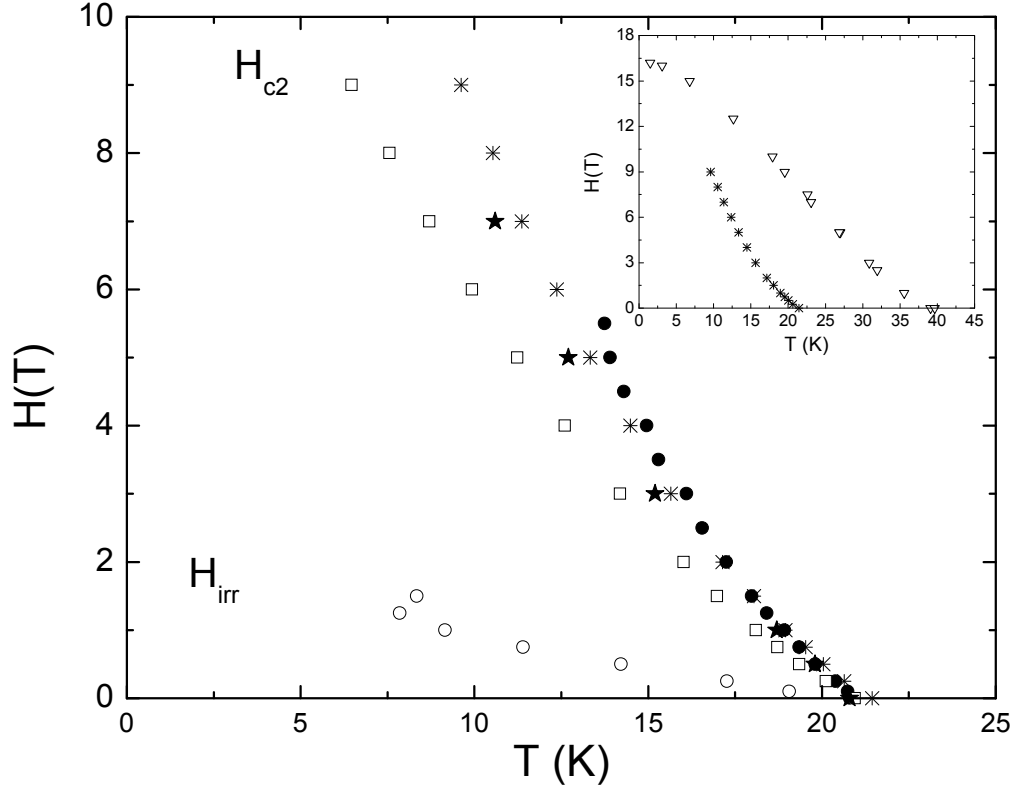
Fig. 9. Upper critical field and irreversibility line for $Mg(B_{0.8}C_{0.2})_2$ — 1100°C/24h sample. For H_{c2}: filled circles - from magnetization, asterisks - from onset criterion of magnetotransport data, squares - from $R = 0$ criterion of magnetotransport data and stars - from heat capacity. Inset: comparison of H_{c2} for pure MgB_2 [6] (open triangles) and carbon doped sample.
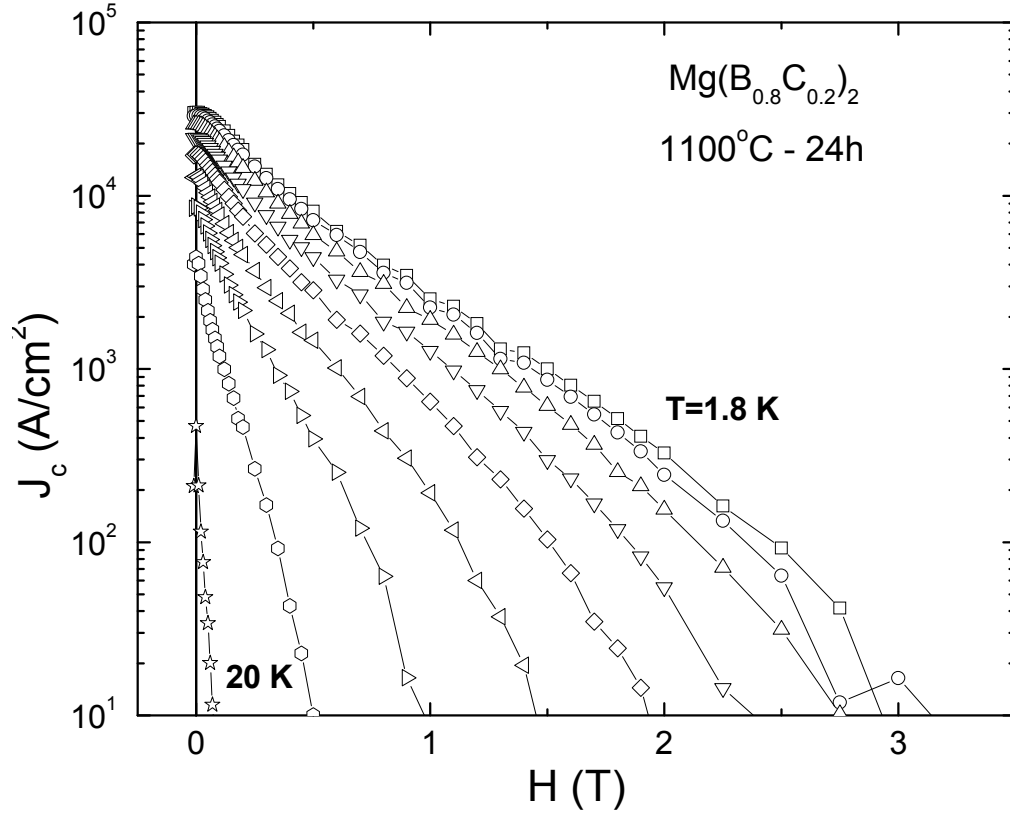
Fig. 10. Critical current density for $Mg(B_{0.8}C_{0.2})_2$ — 1100°C/24h sample as inferred from magnetization loops. Temperatures, from right to left: 1.8, 3, 5, 7.5, 10, 12.5, 15, 17.5, $20K$.
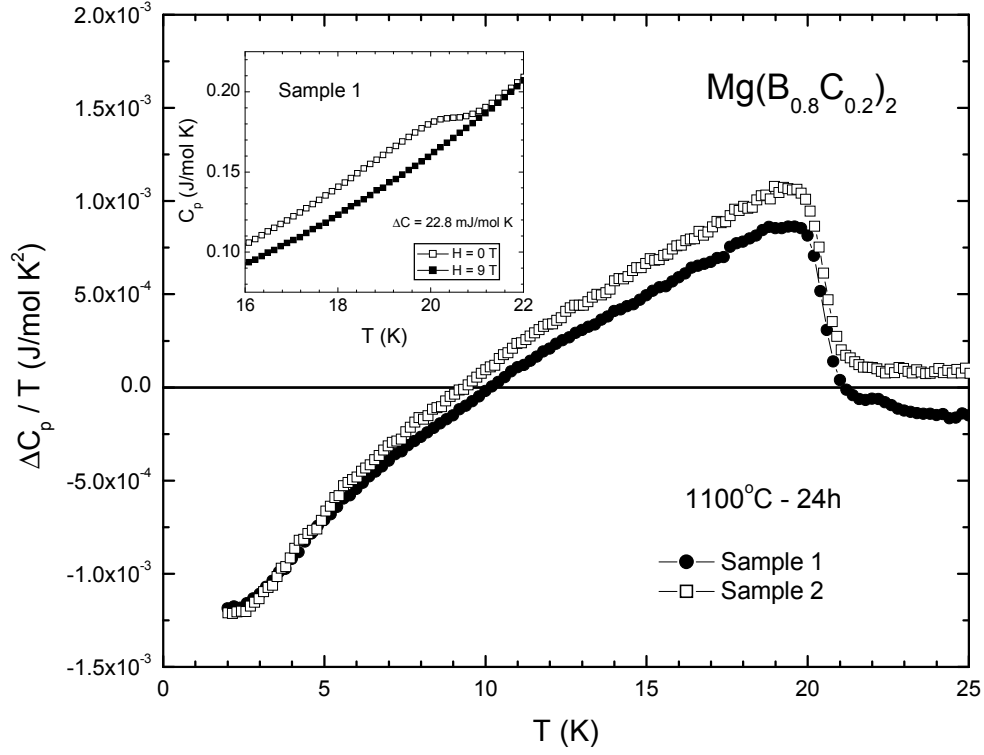
Fig. 11. Heat capacity difference $\Delta C_p/T = (C_p(H=0) - C_p(9T))/T$ as a function of temperature for two different $\text{Mg}(\text{B}_{0.8}\text{C}_{0.2})_2$ — 1100°C/24h samples. Inset: $C_p(T)$ data for $H = 0$ and $H = 9$ T in the region near T_c.

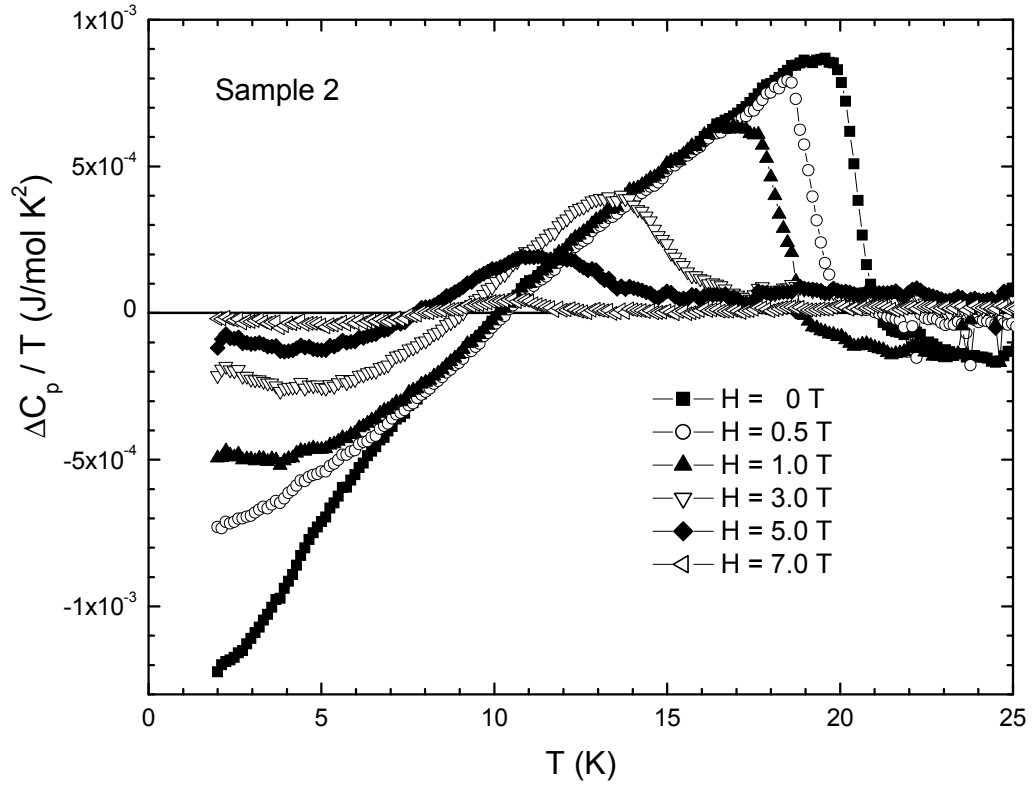Fig. 12. Heat capacity difference $\Delta C_p/T = (C_p(H) - C_p(9T))/T$ as a function of temperature for $\mathrm{Mg(B_{0.8}C_{0.2})_2}$ — $1100^\circ\mathrm{C}/24\mathrm{h}$ sample taken for different applied fields.
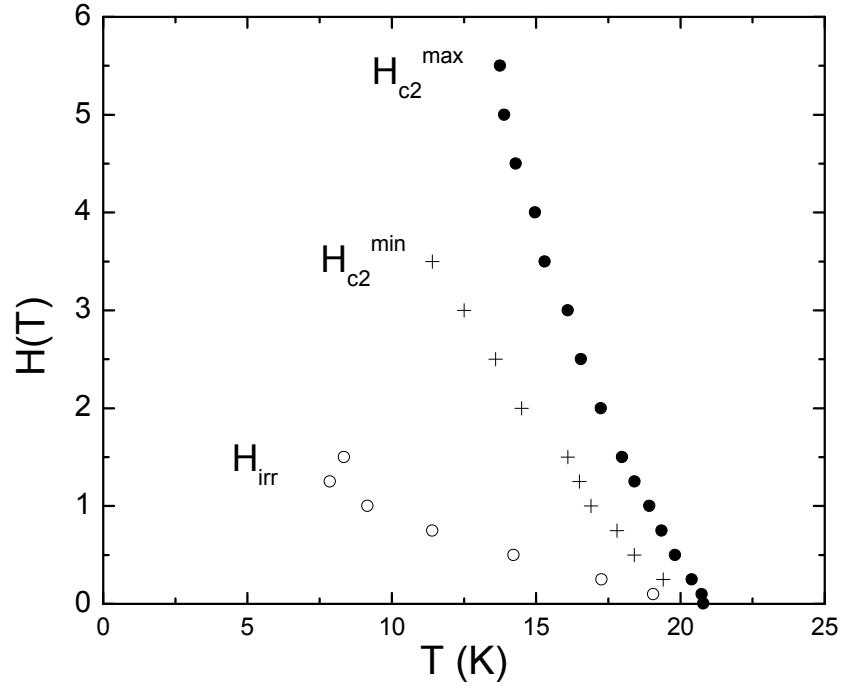
Fig. 13. Anisostropic H_{c2} and irreversibility line H_{irr} curves for $Mg(B_{0.8}C_{0.2})_2$ — 1100°C/24h sample.